LOCKHEED MARTIN ENERGY RESEARCH LIBRARIES
3 4456 0513333 4
CENTRAL RESEARCH LIBRARY
- DOCUMENT COLLECTION

OAK RIDGE NATIONAL LABORATORY

operated by

UNION CARBIDE CORPORATION
NUCLEAR DIVISION

for the

U.S. ATOMIC ENERGY COMMISSION

ORNL-TM-1786

VAPORIZATION PHENOMENA OF HAYNES ALLOY NO. 25 TO 1150°C

D. T. Bourgette

OAK RIDGE NATIONAL LABORATORY
CENTRAL RESEARCH LIBRARY
DOCUMENT COLLECTION
LIBRARY LOAN COPY
DO NOT TRANSFER TO ANOTHER PERSON
If you wish someone else to see this document, send in name with document and the library will arrange a loan.

NOTICE This document contains information of a preliminary nature and was prepared primarily for internal use at the Oak Ridge National Laboratory. It is subject to revision or correction and therefore does not represent a final report.

LEGAL NOTICE

This report was prepared as an account of Government sponsored work. Neither the United States, nor the Commission, nor any person acting on behalf of the Commission:

A. Makes any warranty or representation, expressed or implied, with respect to the accuracy, completeness, or usefulness of the information contained in this report, or that the use of any information, apparatus, method, or process disclosed in this report may not infringe privately owned rights; or

B. Assumes any liabilities with respect to the use of, or for damages resulting from the use of any information, apparatus, method, or process disclosed in this report.

As used in the above, "person acting on behalf of the Commission" includes any employee or contractor of the Commission, or employee of such contractor, to the extent that such employee or contractor of the Commission, or employee of such contractor prepares, disseminates, or provides access to, any information pursuant to his employment or contract with the Commission, or his employment with such contractor.

ORNL-TM-1786

Contract No. W-7405-eng-26

METALS AND CERAMICS DIVISION

VAPORIZATION PHENOMENA OF HAYNES ALLOY NO. 25 TO 1150°C

D. T. Bourgette

MAY 1967

OAK RIDGE NATIONAL LABORATORY
Oak Ridge, Tennessee
operated by
UNION CARBIDE CORPORATION
for the
U.S. ATOMIC ENERGY COMMISSION

LOCKHEED MARTIN ENERGY RESEARCH LIBRARIES

3 4456 0513333 4

CONTENTS

	Page
Abstract	1
Introduction	1
Experimental	2
Sample Preparation	2
Evaporation Apparatus	3
Results and Discussion	4
Validity of the Experimental Technique	4
Alloy Evaporation	5
Identification of Evaporated Elements	5
Metallography	7
Evaporation Behavior of Polished Specimens	11
Conclusions	15
Acknowledgments	15

VAPORIZATION PHENOMENA OF HAYNES ALLOY NO. 25 TO 1150°C

D. T. Bourgette

ABSTRACT

The evaporation rate of Haynes alloy No. 25 was measured at 870, 930, 980, 1040, 1090, and 1150°C over a pressure range of 6×10^{-10} to 5×10^{-7} torr. Results of long-term tests showed that the evaporation rates were highly temperature sensitive. At constant temperature, the evaporation rate decreased with time. Changes in the composition of vapor deposits and electron probe microanalyses have shown that the higher vapor pressure elements, Mn, Cr, Fe, and Ni, were quickly evaporated from the specimen surfaces, resulting in concentration gradients. Further loss of these elements was dependent on their diffusion rates in the cobalt-tungsten matrix, thereby accounting for the decrease in evaporation rate with time.

The major microstructural changes which are directly attributed to evaporation losses are subsurface and surface-connected void formation, gross surface roughening, and formation of Laves phase at the specimen surfaces. Changes in the bulk alloy composition also resulted in the dissolutioning of Laves phase in the subsurface regions of the specimen.

INTRODUCTION

The future success of space exploration is to a great extent dependent on the development of lightweight, efficient power plants to supply the electrical needs of space vehicles. Design studies[1] at the Oak Ridge National Laboratory have shown that high performances are achievable in a nuclear reactor mated to a Rankin cycle turbine generator system employing potassium as a single working fluid. In addition,

[1]A. P. Fraas, Nucleonics 22, 72 (1964).

liquid-metal corrosion studies[2] have shown that the corrosion resistance of Haynes alloy No. 25 is superior to that of Inconel and type 316 stainless steel. The dissolutive corrosion of Haynes alloy No. 25 does not increase inordinately with increasing temperature, and at higher test temperatures, problems associated with aging embrittlement and fatigue cracking are less severe. In addition to the above listed properties the excellent high-temperature strength of this alloy indicates its potential as a container material for boiling potassium at 1000°C.

The room-temperature embrittlement usually associated with this alloy results from the precipitation of a Laves phase; however, this embrittlement is rarely retained above 550°C (ref. 3). The embrittlement does not appear to be more acute in welded than in wrought material; however, compositional changes involving an increase in tungsten and silicon and a decrease in iron and nickel promote the formation of the Laves phase.

The purpose of this investigation was to determine the high-vacuum stability of Haynes alloy No. 25 over its useful temperature range with regard to (1) its evaporation characteristics, (2) the effects of evaporation losses on alloy composition, and (3) the effects of long-term annealing and evaporation losses on the alloy microstructure.

EXPERIMENTAL

Sample Preparation

Specimen stock 0.16 cm thick was cold rolled to approximately 0.015 cm. Specimens with a total area of about 13 cm^2 were cut, polished through 4/0 abrasive paper, degreased, weighed, and their geometric surface area determined. The composition of the alloy used in this study is:

---

[2]D. H. Jansen and E. E. Hoffman, Type 316 Stainless Steel, Inconel, and Haynes Alloy No. 25 Natural-Circulation Boiling-Potassium Corrosion Test Loops, ORNL-3970 (June 1965).

[3]S. T. Wlodek, Embrittlement of a Co-Cr-W (L-605) Alloy, R 61 FPD 538 (Dec. 1, 1961).

Element	Concentration (wt %)
Cr	20.00
W	16.45
Ni	10.97
Fe	1.65
Mn	1.38
Si	0.30
C	0.066
Co	49.16

Evaporation Apparatus

The two types of evaporation apparatus employed in this study are schematically illustrated in Fig. 1. The first apparatus permitted continuous measurement of the evaporation losses by observing the weight change in a specimen suspended from a calibrated steel spring. The combined sensitivity of the spring and the cathetometer for detecting weight changes was 0.004 mg. This apparatus was capable of 5×10^{-9} torr at temperatures to 950°C and 5×10^{-8} torr at 1100°C.

A knowledge of the behavior of the principal elements vaporizing from the alloy is important in understanding the time-dependent changes in evaporation rates and the resulting microstructure of the alloy. Therefore, a second apparatus was designed to permit the collection of vapor deposits under variable conditions of time and temperature. The vapor deposits from induction-heated specimens were quantitatively analyzed for elemental concentrations. This apparatus was capable of 10^{-9} torr at temperatures to 1500°C. The construction, operating characteristics, and experimental procedure for both types of equipment have been discussed previously in detail.[4]

In an effort to determine composition gradients across the specimen thickness, electron probe microanalyses were completed using a Norelco AMR/3 electron probe analyzer. A computer code described by

---

[4]D. T. Bourgette, Evaporation of Iron-, Nickel-, and Cobalt-Base Alloys at 760 to 980°C in High Vacuums, ORNL-3677 (November 1964).

ORNL-DWG 63-4781R2

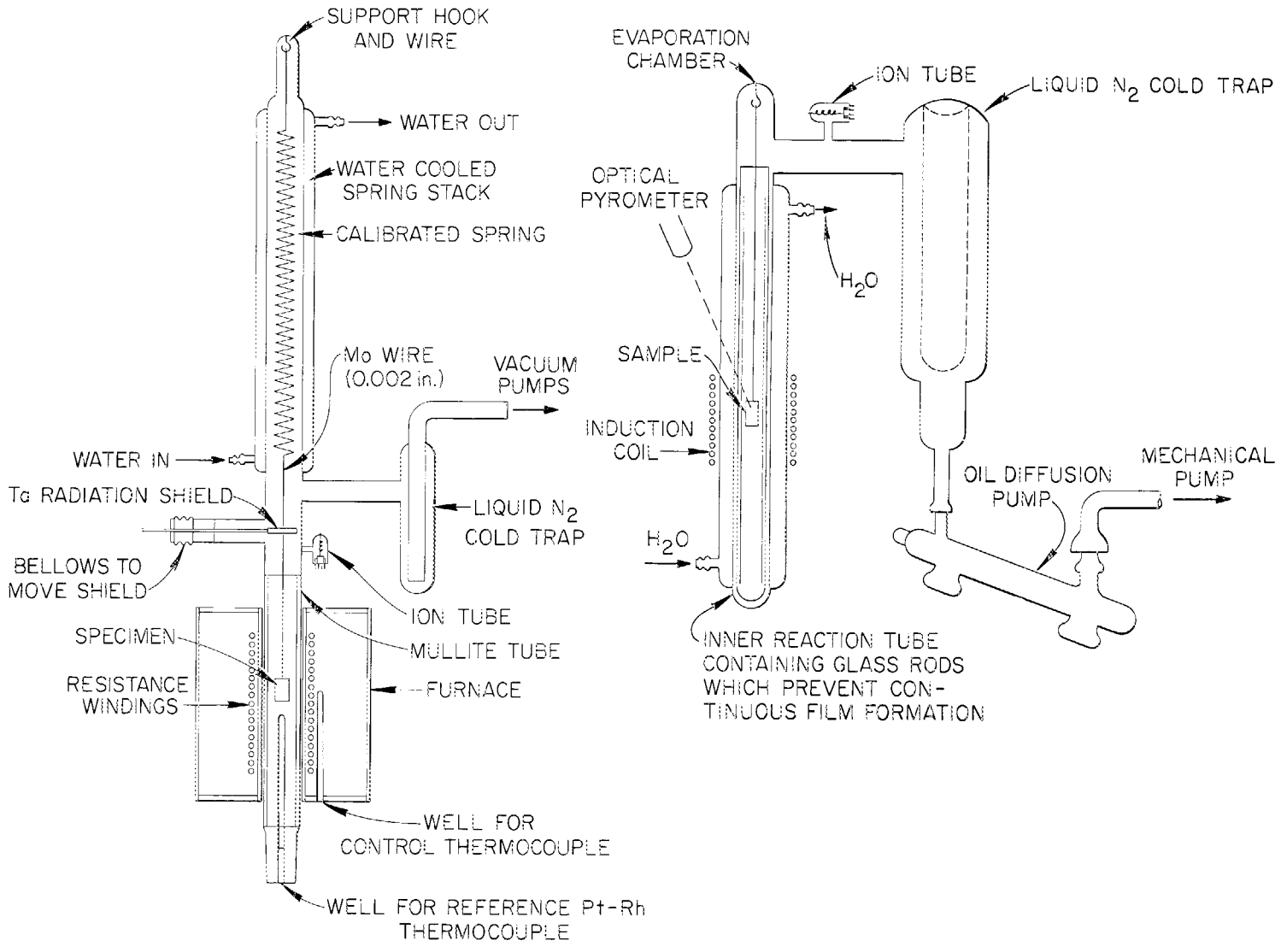

Fig. 1. Schematic Drawings of Evaporation Apparatus Utilized in the Vaporization Studies of Haynes Alloy No. 25.

Brown[5] was used to correct the intensity data for absorption and fluorescent effects and to convert the corrected rate data to weight percents.

RESULTS AND DISCUSSION

Validity of the Experimental Technique

The accuracy of the experimental evaporation technique used in this investigation was verified by the determination of the vapor pressures of pure iron and pure nickel using the Knudsen-Langmuir equation with the vaporization coefficient equal to unity. The measured vapor pressures agreed well with published values. In the case of nickel, the experimental value of 2.25×10^{-7} torr is compared with the published value[6] of 3.00×10^{-7} torr at 1038°C, while for iron an experimental value of 1.54×10^{-7} torr is compared to a published value[7] of 1.77×10^{-7} torr at 872°C. The results of these evaporation tests show a linear weight loss with time, a behavior characteristic of pure metals.[8]

Alloy Evaporation

Identification of Evaporated Elements

Chemical analyses of deposited metal vapors from tests conducted for approximately 500 hr are summarized in Table 1. Although the total amount of material being evaporated increased with increasing temperature, the relative concentrations of the different alloying elements varied considerably. The concentration of the higher vapor pressure elements,

---

[5]J. D. Brown, A Computer Program for Electron Probe Microanalysis, Bureau of Mines No. 6648, 1965.

[6]J. E. Elliott and M. Gleiser, Thermochemistry for Steelmaking, Vol. 1, p. 270, Addison-Wesley, Reading, Massachusetts, 1960.

[7]E. A. Gulbransen and K. F. Andrew, Trans. Met. Soc. AIME 221, 1247 (1961).

[8]J. P. Hirth and G. M. Pound, J. Phys. Chem. 64, 619 (1960).

Table 1. Chemical Analyses of Vapor Deposits Evaporated from Haynes Alloy No. 25

Test Conditions[a]	Actual Weight Loss[b] (mg)	Analyses of Vapor Deposits														Total Vapor Deposit[c] (mg)
		Cr		Mn		Co		Fe		Ni		Si		W		
		(mg)	(wt %)	(mg)	(wt %)	(mg)	(wt %)	(mg)	(wt %)	(mg)	(wt %)	(mg)	(wt %)	(mg)	(wt %)	
872°C for 504 hr	3.40	2.11	66.88	0.56	17.75	0.26	8.27	0.18	5.70	0.03	1.01	0.001	0.03	0.01	0.35	3.155
927°C for 507 hr	4.70	3.08	66.31	0.68	14.64	0.48	10.33	0.17	3.66	0.21	4.52	0.001	0.02	0.024	0.52	4.645
982°C for 509 hr	11.80	7.63	66.58	1.24	10.82	1.75	15.27	0.38	3.32	0.28	2.41	0.15	1.31	0.03	0.29	11.46
1038°C for 505 hr	23.6	14.90	64.50	2.18	9.44	4.43	19.18	0.79	3.42	0.65	2.81	0.08	0.35	0.07	0.30	23.10
1093°C for 503 hr	303.90	146.50	47.79	17.10	5.58	106.0	34.58	9.00	2.94	26.60	8.68	0.94	0.30	0.41	0.13	306.55

[a]At 1×10^{-9} torr.

[b]Initial sample weight minus final sample weight.

[c]Weight of deposit determined by analytical chemistry methods.

Cr, Mn, and Fe, in the vapor deposit decreased with increasing temperature between 872 and 1093°C, while the concentration of the lower vapor pressure elements, Co, Ni, and Si, showed an increase.

Tests conducted at 982°C for times ranging from 5 to 500 hr showed that the concentration of manganese and iron in the deposit decreased with increasing time, while the concentrations of the remaining elements in the deposit increased. The concentration of chromium and cobalt increased at a significantly greater rate than did nickel and silicon. These results indicated a selective loss of alloying elements, resulting in a constantly changing surface composition.

Electron probe microanalysis of specimens tested at temperatures ranging from 872 to 1150°C for times to 3000 hr showed the existence of concentration gradients which varied with time and temperature. Typical results as illustrated in Fig. 2 for a 1040°C test substantiated the

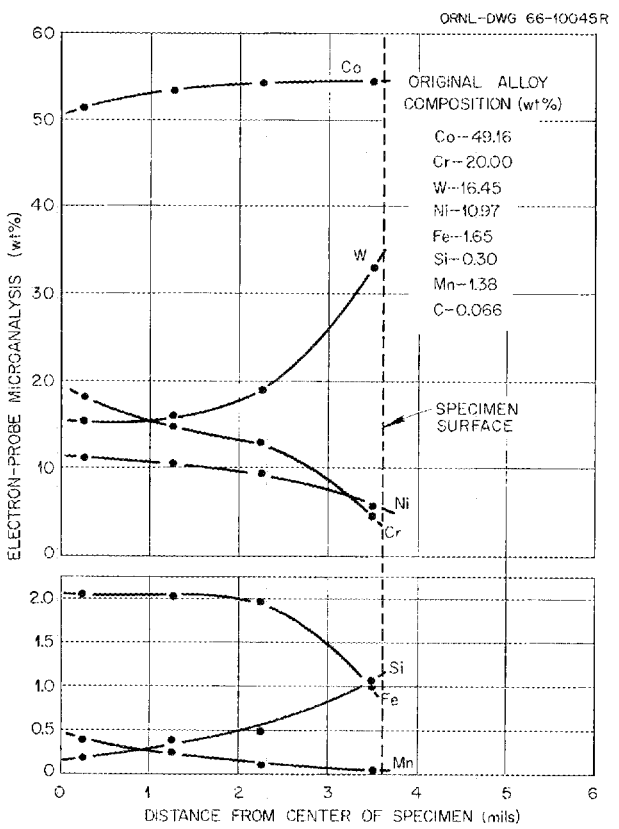

Fig. 2. Composition Profile of a Haynes Alloy No. 25 Specimen Evaporation Tested at 1040°C for 2672 hr.

chemical analysis and indicated that there is a depletion at the specimen surfaces of Fe, Cr, Ni, and Mn. The surface concentration of tungsten and silicon increased substantially, while the cobalt concentration increased only slightly. Further, losses of the higher vapor pressure elements, chromium and manganese, from the interior regions of the specimen resulted in an increase in the Co, W, and Fe concentrations in these regions. This behavior indicated that subsequent losses of the evaporating elements were diffusion-rate dependent.

Metallography

The microstructure of Haynes alloy No. 25 at the temperatures investigated exhibited four major changes that can be directly attributed to evaporation losses. These changes are listed below.

1. The formation of microscopic subsurface voids resulting from the coalescence of Kirkendall vacancies.
2. The formation of a "honeycomb" structure at specimen surfaces above 1000°C.
3. Formation of the Laves phase $(Co,Ni)_2(W,Cr)$ at specimen surfaces.
4. Dissolutioning of the Laves precipitate in the subsurface regions of the specimens due to bulk compositional changes.

These microstructural changes are illustrated in Figs. 3 and 4.

Wlodek[9] reported that Haynes alloy No. 25 on prolonged exposure in the temperature range of 650 to 1100°C will precipitate a Laves phase, which promotes alloy embrittlement. Maximum Laves precipitation occurs in the vicinity of 870°C after about 1000 hr. Aging treatments at higher temperatures result in lesser amounts of Laves phase in the microstructure. Wlodek further stated that silicon stabilizes the Laves phase and also the hexagonal-close-packed modification of the cobalt matrix. Other constituents such as iron and nickel tend to stabilize the face-centered cubic high-temperature structure of the cobalt matrix. In addition, nickel tends to decrease the stability of the Laves phase.

---

[9]S. T. Wlodek, Embrittlement of a Co-Cr-W (L-605) Alloy, R 61 FPD 538 (Dec. 1, 1961).

PHOTO 84999

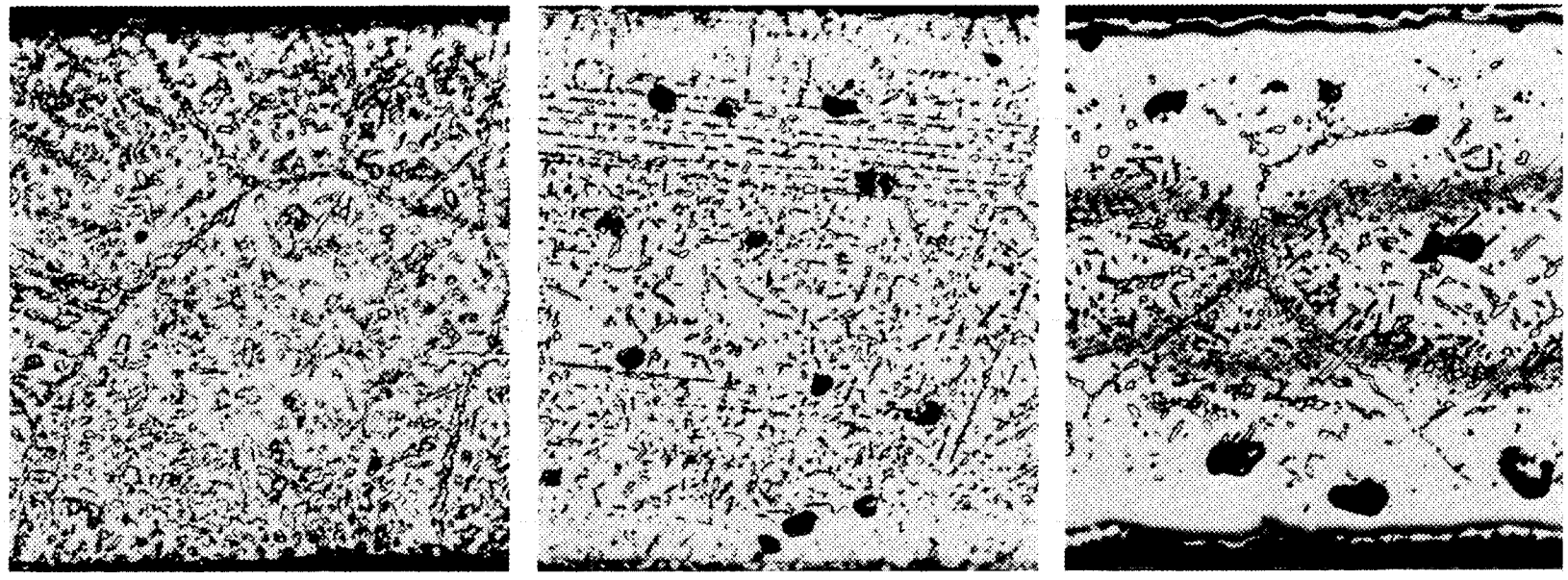

870°C Y-70344 930°C Y-70339 980°C Y-70338

1142 hr 2043 hr 2157 hr

WT. LOSS—0.68 mg/cm^2 WT. LOSS—3.41 mg/cm^2 WT. LOSS—8.73 mg/cm^2

Fig. 3. The Effect of Evaporation Losses of Less Than 10 mg/cm^2 on the Microstructure of Haynes Alloy No. 25. Original magnification 500X. Etchant: 100 ml H_2O + 40 ml $HC_2H_3O_2$ + 40 ml HCl + 15 ml H_2SO_4 + 40 ml HNO_3 + 25 g $FeCl_3$, electrolytically polished using a platinum cathode.

PHOTO 84998

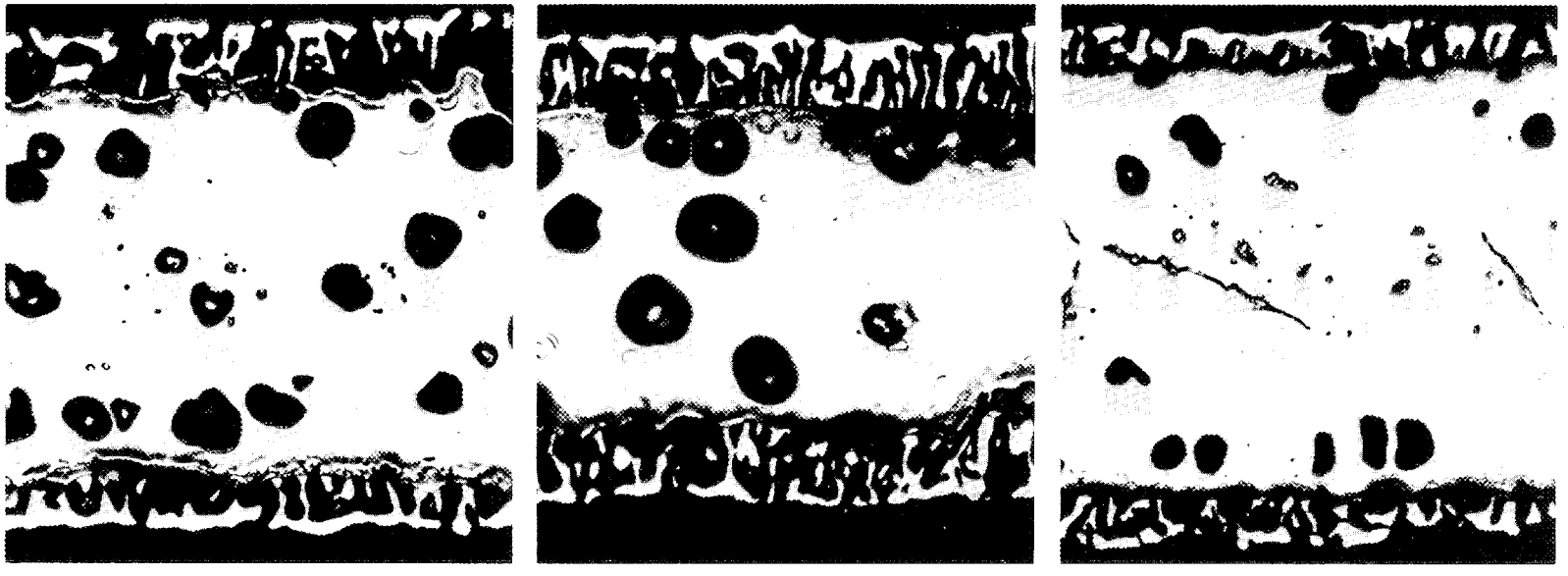

1040°C Y-70343 1090°C Y-70342 1150°C Y-70341

2672 hr 670 hr 164 hr

WT. LOSS—22.6 mg/cm^2 WT. LOSS—27.5 mg/cm^2 WT. LOSS—25.20 mg/cm^2

Fig. 4. The Effect of Evaporation Losses in Excess of 20 mg/cm^2 on the Microstructure of Haynes Alloy No. 25. Original magnification 500X. Etchant: electrolytically polished using a platinum cathode in a solution of 100 ml H_2O + 40 ml $HC_2H_3O_2$ + 40 ml HCl + 40 ml HNO_3 + 25 g $FeCl_3$.

Slight compositional changes involving the elimination of silicon, a decrease in the tungsten level, and an increase in the iron and nickel contents may suppress the Laves phase precipitation in the temperature range 850 to 1000°C. This study has shown, however, that in addition to chromium and manganese, substantial amounts of iron and nickel with lesser amounts of silicon were evaporated from the specimen surfaces. The loss of these elements from the surfaces of thin specimens, in essence, resulted in an increase in the concentration of tungsten and cobalt. This evaporation behavior could therefore promote the formation of the Laves phase at temperatures above 900°C. Wlodek[9] also reported that Laves phase forms within 64 hr at temperatures of 760 to 980°C. Evaporation tests have shown, however, that at these temperatures far longer times are required to substantially change the bulk composition of the alloy. Therefore, the Laves phase in the microstructure (Fig. 3) resulted from thermal effects and not from evaporation.

Results of x-ray diffraction analysis showed that the surfaces of all specimens evaporation tested at 930 to 1150°C were composed of the Laves phase. Metallographic examination further showed that the amount of Laves phase at the specimen surfaces increased with temperature or with an increase in evaporation losses. This behavior is illustrated in Fig. 3 for evaporation losses of less than 10 mg/cm^2 and in Fig. 4 for losses in excess of 20 mg/cm^2. Dissolution of the Laves phase in the subsurface regions occurred simultaneously with its formation on the surface. This anomalous behavior is attributed to the gross differences in composition in these regions due to evaporation losses of the higher vapor pressure elements, Mn, Cr, and Si.

The higher evaporation losses from regions near the surface and the coalescence of voids directly beneath the surface resulted in the honeycomb structure at the specimen surfaces (Fig. 4). Subsurface voids were present throughout the microstructure of the 0.015-cm specimens that had suffered a weight loss of 2 mg/cm^2 or greater. The formation of these microscopic voids is attributed to the coalescence of Kirkendall vacancies.

Evaporation Behavior of Polished Specimens

Evaporation tests were conducted at 870, 930, 980, and 1040°C for times ranging from 1200 to 2700 hr. Tests conducted at 1090 and 1150°C were terminated prematurely at 650 and 170 hr because of excessive evaporation losses. The results of these tests, illustrated in Fig. 5, show that evaporation losses in this alloy are highly dependent on temperature. In addition, the changes in slope of these curves indicate a decrease in the evaporation rate with increasing time. This behavior is illustrated more clearly in Fig. 6. The decrease in evaporation rate with time was greater at the low temperatures and is attributed to the decrease in diffusion rates of the evaporating elements at these temperatures.

As shown earlier by the existence of concentration gradients and the time-dependent changes in the composition of vapor deposits, the surfaces of the specimens become depleted in the higher vapor pressure elements. Therefore, their future losses become diffusion-rate dependent. The major significance of Fig. 6, however, is that the curves are nearly parallel which indicate that the evaporation mechanisms or the rate controlling step changes only slightly between 2 and 1000 hr. It is postulated that this change may be due to the formation of Laves phase on the specimen surfaces.

Potential space applications for Haynes alloy No. 25 may require service lives in excess of 10,000 hr. A method for predicting total weight losses for potential operating temperatures to various service lives is plotted in Fig. 7. In addition, these curves may be used to select operating temperatures for a maximum tolerable weight loss. The microstructures associated with such weight losses may in turn be estimated with the aid of Figs. 3 and 4. It is emphasized, however, that this research tested specimens only 0.015 to 0.020 cm in thickness and that greater thicknesses might yield quite different experimental results. It is felt that the major differences would be an increase in the severity of the concentration profiles of the evaporating elements near the surfaces and a decrease in the severity of void formation within the bulk of the sample. However, the evaporation rates would

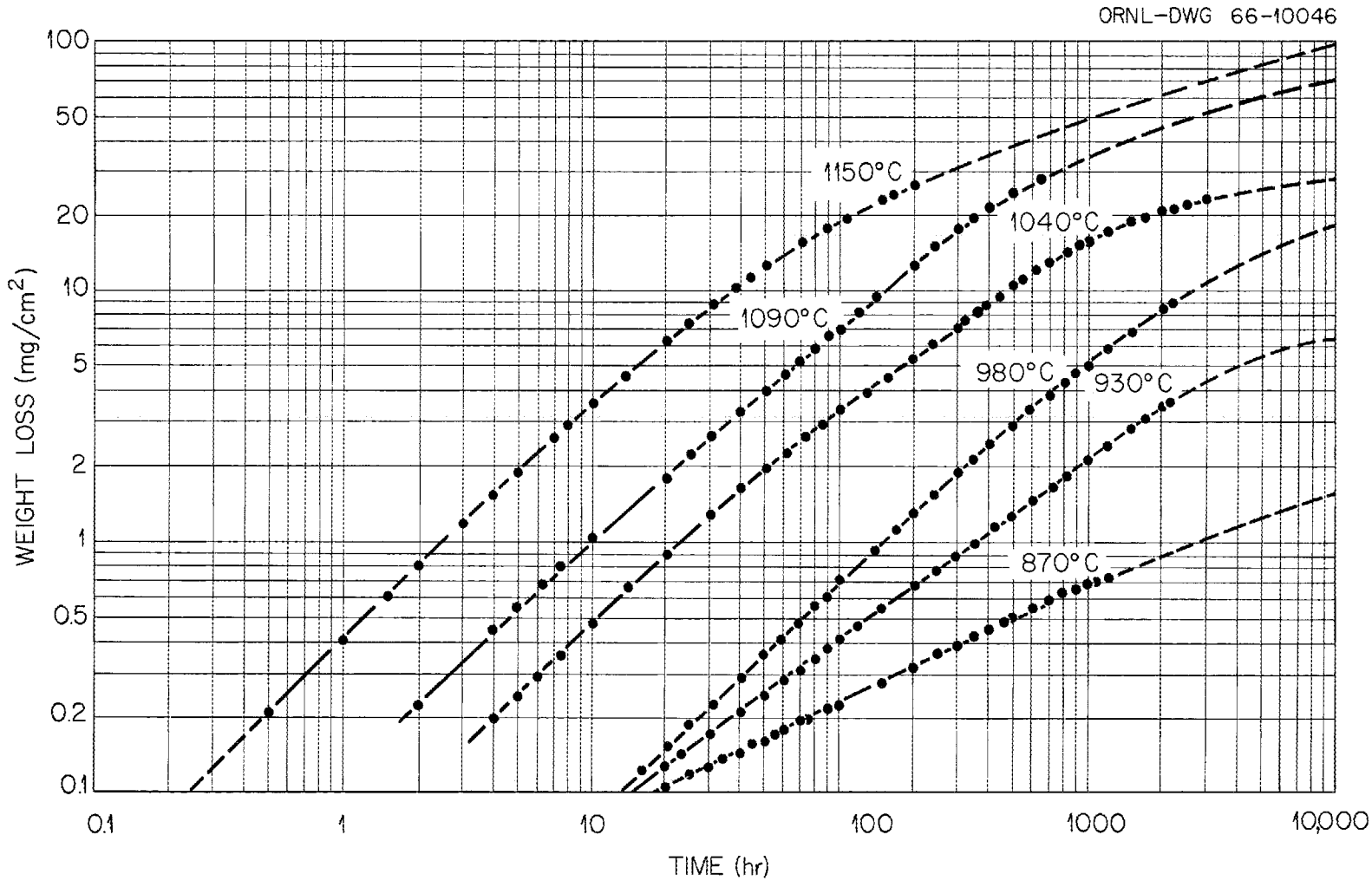

Fig. 5. Evaporation Losses of Haynes Alloy No. 25 at Pressure of 10^{-8} to 10^{-9} torr.

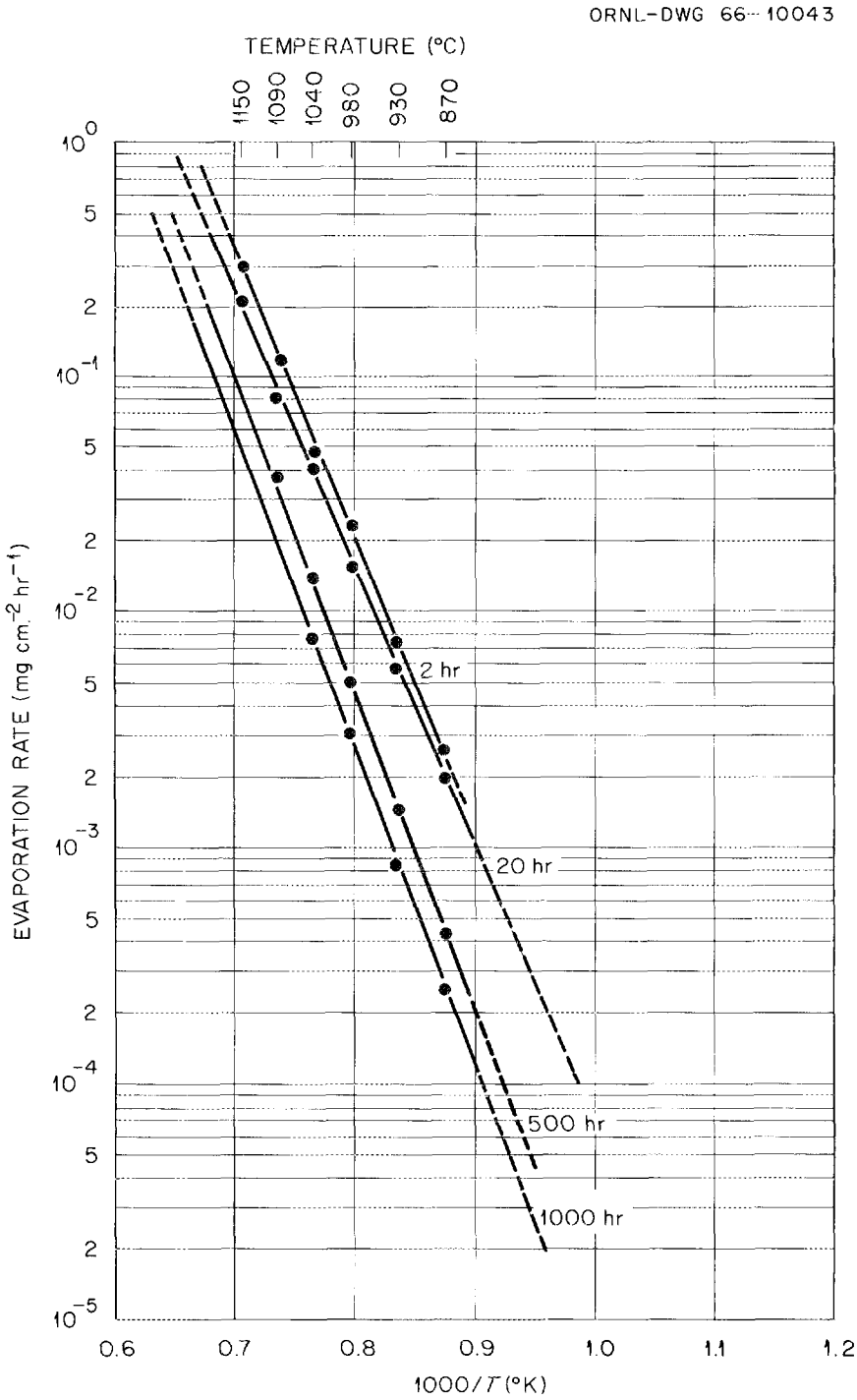

Fig. 6. Variations in the Evaporation Rate of Haynes Alloy No. 25 with Time and Temperature.

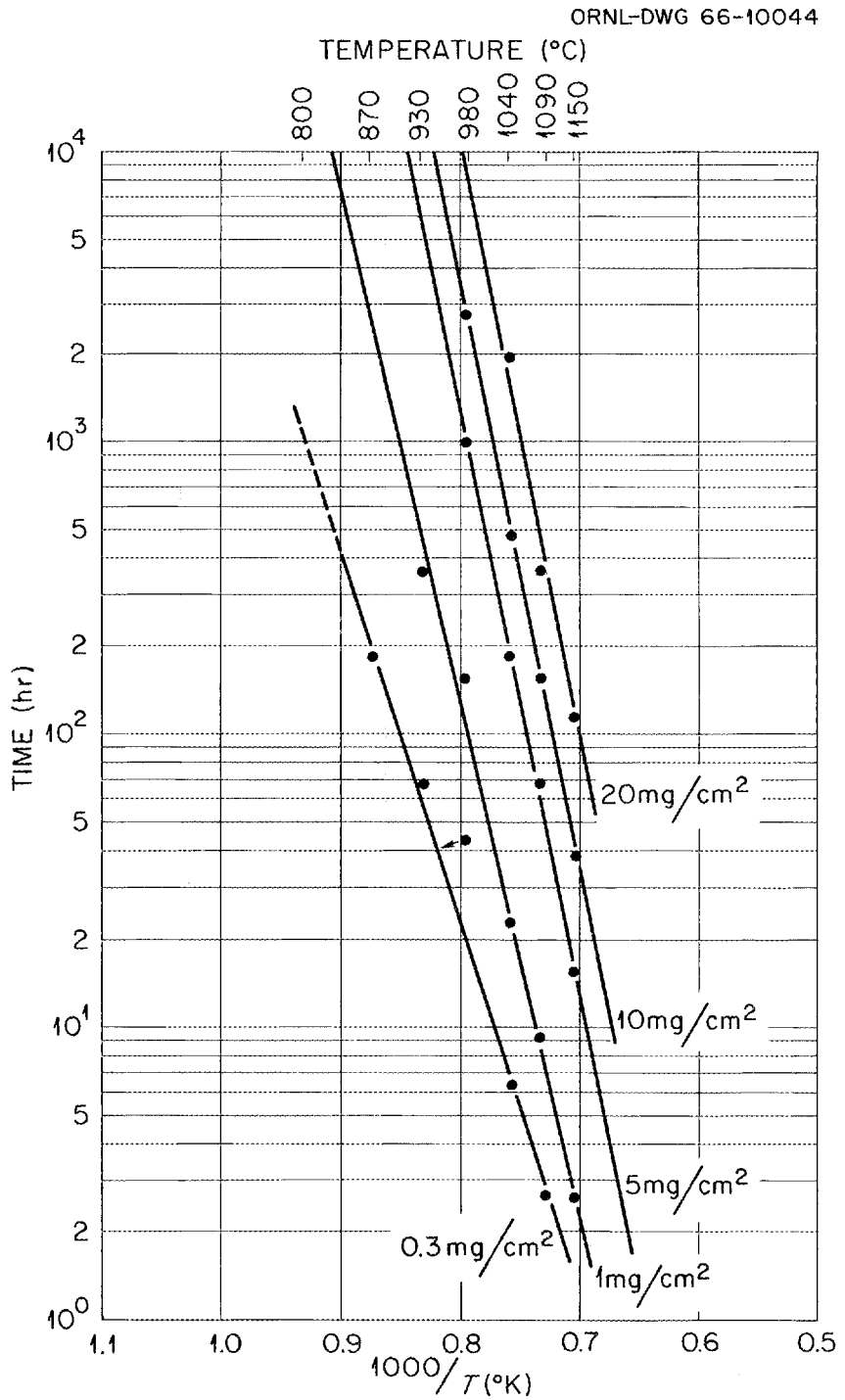

Fig. 7. The Effect of Temperature on the Time Necessary to Evaporate a Known Quantity of Material from Haynes Alloy No. 25.

remain relatively high as long as the temperature was sufficient for the higher vapor pressure elements to diffuse to the specimen surfaces. Greater thicknesses simply mean that more material is available for selective evaporation.

CONCLUSIONS

This study has shown that the higher vapor pressure alloying elements, manganese and chromium, were selectively evaporated from Haynes alloy No. 25 at high vacuum in the temperature range of 870 to 1150°C. When the surface of this cobalt-base alloy became depleted of the higher vapor pressure alloying elements, their further loss became dependent on their diffusion rates in the base alloy. At the lower temperatures (<1050°C), the low diffusion rates of the volatile, evaporating elements resulted in severe concentration gradients. At temperatures of 1090 and 1150°C these gradients were less severe; however, there occurred a much greater change in the bulk concentration of these higher vapor pressure elements. Eventually, the specimen surfaces became enriched in the lower vapor pressure elements, cobalt and tungsten. Because of this behavior, the evaporation rate at constant temperature decreased with time. The amount of cobalt in the vapor increased with time.

Surface roughening, void formation, and formation of massive Laves phase at the specimen surfaces were the major microstructural changes attributed to evaporation losses. As evaporation of the higher vapor pressure elements continued, however, the alloy composition in the subsurface regions of the specimens was altered in a manner which resulted in the dissolution of the finer Laves precipitate.

The use of Haynes alloy No. 25 in space environments for times in excess of 10,000 hr is not recommended at temperatures above 870°C. It is felt at the present time that thicker sections could be used successfully at 800°C or below.

ACKNOWLEDGMENTS

The author is indebted to the many service departments in carrying out various phases of these experiments. The assistance of W. R. Laing

of the Analytical Chemistry Division for the chemical analysis proved to be necessary services in the interpretation of these experiments. Discussions with H. Inouye of the Metals and Ceramics Division were instrumental in the formulation of the conclusions reached in this investigation.

INTERNAL DISTRIBUTION

1–3. Central Research Library
4. Reactor Division Library
5–6. ORNL – Y-12 Technical Library Document Reference Section
7–21. Laboratory Records
22. Laboratory Records, ORNL R.C.
23. ORNL Patent Office
24. G. M. Adamson, Jr.
25. S. E. Beall
26. R. J. Beaver
27–31. D. T. Bourgette
32. G. E. Boyd
33. F. L. Culler
34. J. E. Cunningham
35. J. H. DeVan
36. J. R. DiStefano
37. R. G. Donnelly
38. A. P. Fraas
39. J. H Frye, Jr.
40. J. M. Googin (Y–12)
41. R. J. Gray
42. W. R. Grimes
43. A. G. Grindell
44. W. O. Harms
45–47. M. R. Hill
48. H. W. Hoffman
49. H. Inouye
50. C. E. Larson (Y-12)
51. C. F. Leitten, Jr.
52. H. G. MacPherson
53. R. E. MacPherson
54. R. W. McClung
55. H. E. McCoy
56. R. E. McDonald
57. D. L. McElroy
58. C. J. McHargue
59. A. J. Miller
60. P. Patriarca
61. R. A. Robinson
62. J. E. Savolainen
63. J. L. Scott
64. G. M. Slaughter
65. S. H. Smiley (K-25)
66. R. L. Stephenson
67. R. W. Swindeman
68. R. L. Wagner
69. A. M. Weinberg
70. J. R. Weir, Jr.

EXTERNAL DISTRIBUTION

71. G. M. Anderson, AEC, Washington
72. C. H. Armbruster, Wright-Patterson AFB
73–75. V. P. Calkins, General Electric, NMPO
76. B. W. Colston, USAEC, Germantown, Maryland
77. D. F. Cope, RDT, OSR, AEC, Oak Ridge National Laboratory
78. J.W.R. Creagh, NASA, Lewis Research Center
79. J. Davis, Jet Propulsion Laboratory
80. R. W. Dayton, Battelle Memorial Institute
81. D. DeHalas, Pacific Northwest Laboratory, Richland, Washington
82. G. K. Dicker, AEC, Washington
83. E. M. Douthett, AEC, Washington
84. J. K. Elbaum, Code MAMP, Wright-Patterson AFB
85. D. C. Goldberg, Westinghouse Astronuclear Laboratory
86. J. L. Gregg, Bard Hall, Cornell University
87–88. D. H. Gurinsky, Brookhaven National Laboratory
89. R. Hall, NASA, Lewis Research Center
90. R. C. Hamilton, Institute for Defense Analyses, 1666 Connecticut Avenue, N.W., Washington, D.C.

91. E. E. Hoffman, General Electric, Cincinnati
92. D. Johnson, Sandia Corporation, Albuquerque, New Mexico
93. J. S. Kane, University of California
94. W. J. Larkin, AEC, Oak Ridge Operations
95. J. J. Lombardo, NASA, Lewis Research Center
96. J. J. Lynch, NASA, Washington
97. T. P. Moffitt, NASA, Lewis Research Center
98–100. T. A. Moss, NASA, Lewis Research Center
101. R. A. Noland, Argonne National Laboratory
102. Louis Rosenblum, NASA, Lewis Research Center
103. N. D. Sanders, NASA, Lewis Research Center
104. H. Schwartz, NASA, Lewis Research Center
105. F. C. Schwenk, AEC, Washington
106–110. J. M. Simmons, AEC, Washington
111. E. E. Stansbury, University of Tennessee
112. D. K. Stevens, AEC, Washington
113. R. L. Stromburg, Sandia Corporation, Albuquerque, New Mexico
114. G. W. Wensch, AEC, Washington
115. M. J. Whitman, AEC, Washington
116. Division of Research and Development, AEC, Oak Ridge Operations
117–131. Division of Technical Information Extension